doi: 10.15407/ujpe62.07.0605

V.G. LITOVCHENKO, T.I. GORBANYUK, V.S. SOLNTSEV

V.E. Lashkaryov Institute of Semiconductor Physics, Nat. Acad. of Sci. of Ukraine
(41, Prosp. Nauky, Kyiv 03028, Ukraine; e-mail: lvg@isp.kiev.ua)

PACS 61.72.uf, 62.23.Eg, 68.43.-h

MECHANISM OF ADSORPTION-CATALYTIC ACTIVITY AT THE NANOSTRUCTURED SURFACE OF SILICON DOPED WITH CLUSTERS OF TRANSITION METALS AND THEIR OXIDES

Mechanisms of adsorption-catalytic activation of composites fabricated on the basis of porous silicon with incorporated nanoparticles of transition metals (Pd, W, Cu) and their oxides have been analyzed theoretically. The influence of adsorbed atoms of acceptor elements (O, S, F, Cl) on the catalytic activity of transition metals during the formation of surface nanoclusters of transition metal oxides is revealed. The enhancement of the catalytic activity of transition metals with the completely filled d-band may consist in a change of the filling of d-states with electrons (the appearance of holes above the Fermi level) at the formation of surface nanoclusters of transition metal oxides. The results of experimental researches of the adsorption-electric effect in gas-sensitive structures with Schottky barriers obtained within the method of high-frequency volt-farad characteristics are presented. The experimental adsorption isotherms of hydrogen and hydrogen sulfide on the surface of nanostructured silicon composites with copper, tungsten, palladium, and their oxides in the pores are analyzed. An increased adsorption sensitivity of those composites to various gases (H_2, H_2S, H_2O) in comparison with an ordinary porous silicon layer is found. It is established that the mechanism of physical adsorption is realized at low gas pressures (≤ 25 ppm) and/or short times of the adsorbate-substrate interaction, and the chemisorption mechanism at higher pressures and in the course of long-term processes. This conclusion agrees with the theoretical data calculated for the adsorption heat from experimental isotherms (0.3–0.5 eV).

K e y w o r d s: nanostructured silicon, nanoparticles, transition metals and their oxides, adsorption sensitivity, hydrogen sulfide, gas sensor.

1. Introduction

Certain types of transition metals (TMs) with the incompletely filled *d*-band and some of their compounds [1–6] are the most active catalytic centers. An important feature of TM-based catalysts consists in that the role of individual catalytically active centers dominates for metals [2], whereas the collective system of electrons has a larger influence on the catalytic activity in semiconductors [1, 2].

In this connection, some challenging problems arise: How crucial for the catalysis are the specific properties of nanoclusters of transition metals in complex compounds? Can TMs with the completely filled *d*-shell be "activated" for catalysis?

Hence, a number of issues can be distinguished, which are to be considered as crucial for the problem of absorption-catalytic processes at transition metals. In particular,

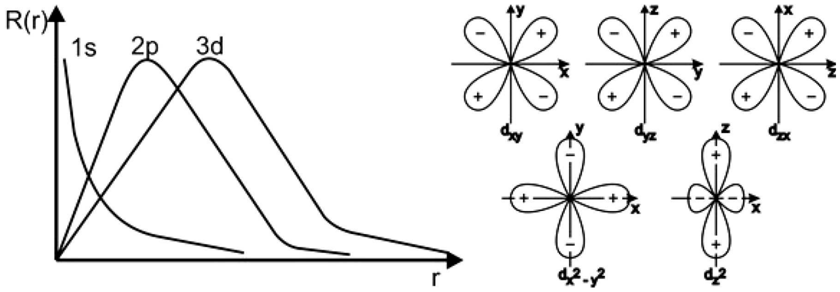

Fig. 1. Schematic diagrams illustrating the angular (d_{xy}, d_{yx}, d_{zx}, ${}^{2}_{dx}{}^{2}_{-y}$, d^2_z) and radial ($R(r)$) distributions of atomic wave functions in the transition metal

1) the crucial role of incompletely filled d-orbitals in catalytic reactions, the account of the varying population of d-shells and their coordination saturation, as well as the states of electron spin pairing;

2) the influence of the internal "crystalline field" and the field formed by the additional component of the cluster (adsorbed atoms/molecules);

3) the role played by oxygen (O) atoms and atoms of other acceptor elements (S, F, Cl) in a change of the filling of d-orbitals in transition metals, if the surface clusters of transition metal oxides (MeO_x) are created, and, hence, in the enhancement of their catalytic activity.

Below, we will analyze how those factors affect the adsorption-catalytic activity of the surface nanoclusters of transition metals and their oxides that are inserted into the pores of the near-surface layer in the porous silicon matrix.

2. Theoretical Analysis of Mechanisms of Absorption-Catalytic Activation of Complex Transition Metal Compounds

External filled electron states in the atoms of transition metals are d-levels. Specific features in the angular and radial distributions of the wave functions of d-orbitals, which distinguish them from s- and p-orbitals, are responsible for specific physical and chemical properties of transition metal atoms, irrespective of whether they are in the crystal bulk or at the crystal surface. The major factor determining the catalytic activity of d-orbitals in transition metals is their elongated spatial configuration (1.5 to 2 times in comparison with s- and p-orbitals) (Fig. 1) [2, 6–8]. In TMs, d-orbitals are external filled valence levels that are active in donor "binding" reactions. If the d-orbitals are partially filled, the atoms becomes active in acceptor reactions, which weaken the interaction between atoms in adsorbed molecules and govern their decomposition, i.e., favor the break of bonds in adsorbed molecules and the appearance of new active radicals.

An important factor is also the account for the influence of the internal crystalline field on the filling of d-orbitals [9–11], which becomes stronger in the case where the molecular structure of a cluster has a more asymmetric geometry (Fig. 2). Qualitatively, this phenomenon can be estimated by calculating the component of the polar bond between TM atoms and the atom of an adsorbed impurity. Using a phenomenological approach, which is based on the Pauling approach, it is possible to calculate the electronegativity difference $\Delta X_{\mathrm{AB}} = X_{\mathrm{A}} - X_{\mathrm{B}}$ between the atoms in the AB cluster. According to Pauling, the ionicity α_p is determined from the ionicities of chemical elements, by using the general relation [12–15]

$$\alpha_p^2 = i, \quad i = [1 - \exp(-\Delta X_{\mathrm{AB}}/2)^2] \approx \Delta X_{\mathrm{AB}}^2/4, \quad (1)$$

$$(i^{1/2}) \approx 1/2(X_{\mathrm{A}} - X_{\mathrm{B}}) \text{ if } \Delta X_{\mathrm{AB}} < 1. \quad (2)$$

The difference $\Delta X_{\mathrm{AB}} = (X_{\mathrm{A}} - X_{\mathrm{B}})$ is proportional to the difference between the atom ionization energies: $\Delta X_{\mathrm{AB}} \sim (\varepsilon_{\mathrm{A}} - \varepsilon_{\mathrm{B}})$ [6–8]. Normalizing this quantity by the interatomic distance, it is possible to estimate the strength of the polar bond, which promotes, under certain conditions, the decay of molecules A_1A_2 on the substrate B and provides the ionization of the complex AB:

$$F = \Delta X_{\mathrm{AB}}/(r_{\mathrm{A}} + r_{\mathrm{B}}).$$

Another method used for the calculation of the energies of ionic and valence bonds in the AB complex consists in the application of the term (orbital) energies ε_{A}, ε_{B}, ε_{C}, and the energies of hybridized orbitals $\varepsilon_{\mathrm{A}}^h$ and $\varepsilon_{\mathrm{B}}^h$ [6, 16–18] of atoms that form chemical bonds:

$$+\varepsilon_{\mathrm{B}}^h = \frac{1}{2}(\varepsilon_{9d}^{+}\varepsilon_{pe} + \varepsilon_d), \quad (3)$$

$$\varepsilon_i = \eta(\varepsilon_{\mathrm{A}}^h - \varepsilon_{\mathrm{B}}^h)/2, \;\; \eta \sim 1.2, \;\; \varepsilon_V = \eta(\varepsilon_{\mathrm{A}}^h + \varepsilon_{\mathrm{B}}^h)/2, \quad (4)$$

$$\alpha_p = \varepsilon_i/(\varepsilon_v^2 + \varepsilon_i^2)^{1/2}, \quad (5)$$

where α_p is the bond ionicity. As follows from Table 1, the values of ionicity a_p calculated by both methods for various TMs turned out close to each other ($< 0.6 \div 0.8$).

The most substantial variation of the TM activity takes place at the electron transitions, when the filling degree of electron d-shells varies, in particular, at the transition of a d-electron on a shell of the adsorbed acceptor impurity atom. In this case, the number of d-electrons decreases from the maximum value $N_d^{\max} = 10$ and becomes equal to nine or less. The resulting complex becomes catalytically active due to the incompletely filled d-shell of TM. The TM atom with the completely filled d-shell (at $N_d = 10$) becomes neutral and similar to the atoms of group VIII in the Periodic system of elements. For instance, for group IV, these are atoms Cu, Zn, Ga, Ge, and others (Table 1).

Palladium (Pd) demonstrates a classical example of how an atom acquires the catalytic d-activity under the influence of a crystalline field. In the isolated atomic state, palladium is catalytically inactive, because it has a completely filled d-orbital ($N_d = 10$). However, under the action of the internal crystalline field and since the energy of the d- and s-levels of Pd atom are close to each other, one of the palladium d-electrons transits onto a higher (but close by energy) s-level (Fig. 3). As a result, the palladium d-orbital becomes only partially filled ($N_d = 9$).

A similar effect of the influence of an internal crystalline field can be used to change the catalytic abilities of other elements as well. By reducing the d-shell occupation number to $N_d = 9$ or 8, we increase the catalytic activity of TMs. On the other hand, the adsorption-catalytic properties of elements can be passivated by adding electrons to the d-shell to obtain $N_d = 10$, but this process is driven by a different mechanism.

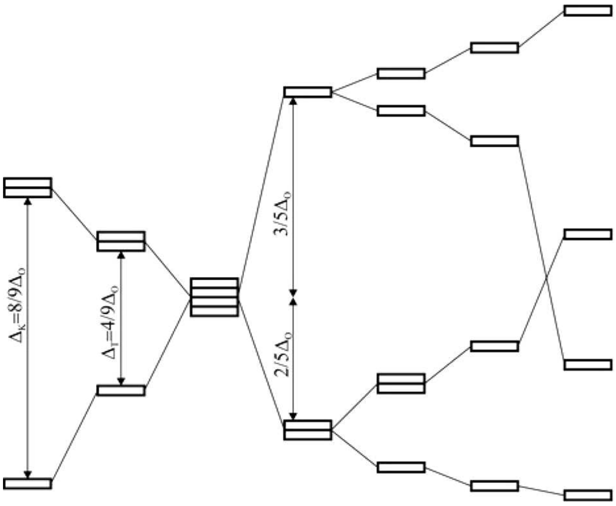

Fig. 2. Splitting of the d-level in the fields with various symmetries [2]: (from left to right) cube, tetrahedron, sphere, octahedron or square pyramid, weakly distorted tetragonal structure, square

Table 1. **Calculated parameters of ionic bonds for transition metals and some A_gB_a pairs using the method of hybrid atomic terms**

N_m period	TM(d)	$A(a)$ electron configu-ration	ε_s	ε_p	ε_d	α_π
III	Cu-$3d^4 4s^2$	(0 $2S^2 2p^4$)	–29.1	7.0 (14.1) 1.8	14	
	Mn $3d^s 4S^2$					
	Fe $3d^6 4S^2$	(F $2S^2 2p^5$)	–36	–17	15.3	
	Co $3d^7 4S^2$	(S $3S^2 3p^4$)	–21	–10.3	16.5	
		Cl $3S^3 p^5$	–24.6	–12.3	78	
	Ni $3d^8 4S^2$		8.4	3.4	19	
	Cu $3d^{10} 4S^1$		7	1.8	20	0.7
	Zn $3d^{10} 4S^2$		8.4	3.4		0.65
	Ga $3d^{10} 4P^1$		11.4	4.9		0.6
	Ge $3d^{10} 4P^2$		14.4	6.4		0.55
	Sc $3d^1 4S^2$				9.3	
	Ti $3d^2 4S^2$				11	
	V $3d^3 4S^2$				12.5	
V	Pd $4d^{10} S$				17.7	
	Ag $4d^{10} 6S^1$				19,2	
Y1	W $5d^4 6S^2$				11	
VI	Pt $5d^9 S^1$				16.5	
	Au $5d^{10} 6S^1$		18	6.5	2.3	

The catalytic activity of complexes changes with the filling of their d-orbitals due to the elimination of a degeneration and the splitting of d-levels under the influence of the crystalline field, which is consider-

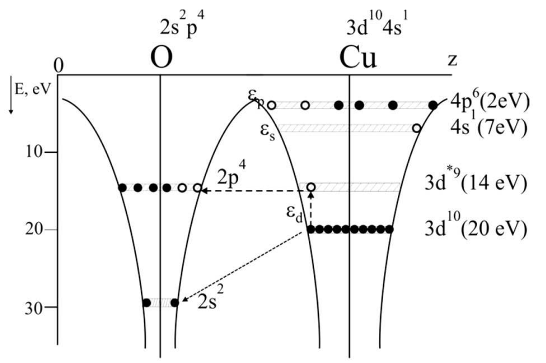

Fig. 3. Electron energy diagram for a Cu–O cluster

ably different for various configurations of the crystal cell in a cluster. As an example, Fig. 2 demonstrates data testifying that both an increase and a decrease of the splitting energy for the degenerate d-orbital in an isolated TM atom are possible [2, 19, 20]. One can see that the symmetric d_{x2-y2} and d_{zy} orbitals become shallower for cubic symmetry, whereas the asymmetric d_{z2}, d_{x2}, and d_{y2} ones are deeper and, thus, more stable.

The strongest splitting (inverse to which is observed in the "spherical" complex) is provided by structures with more asymmetric configurations of the complex and with a low symmetry (a pyramid, a planar configuration). In addition, the energy of orbitals changes at that owing to the spin pairing effect.

The study of "neutral", i.e. non-catalytic, TMs—namely, the elements of groups III, IV, and V with incomplete filling of their d-orbitals, which are located to the left with respect to central elements (with $N_d = 10$) in the Periodic system as their d-orbitals are gradually filled—is also of interest. As was already mentioned, the reactivity of TMs depends on both the depth and the spin saturation of their d-orbitals. In works [2–4], it was emphasized that the TM reactivity depends non-monotonically on the consecutive filling of d-shells. This is a result of the fact that, on the one hand, d-electrons try to become more stable, and, on the other hand, they try to pair (by spins) with one another. In a strong crystalline field, the spin component of the influence decreases. i.e. the influence of the crystalline field dominates.

For each TM, there is a specific type of impurities that provides a high reaction ability, namely, the presence of a non-paired spin configuration. In order to estimate the TM catalytic activity, the following magnitudes of crystalline field $E_{\rm cr}$ in the considered clusters were quoted in work [2]: $E_{\rm cr} \approx 1{\div}2$ eV for 2-valent TMs^{2+}, $E_{\rm cr} \approx 2{\div}3$ eV for 3-valent TMs^{3+}, and $E_{\rm cr} \approx 4{\div}5$ eV for 4-valent TMs^{4+} (in particular, Pt^{4+}), i.e. the predicted values of $E_{\rm cr}$ are rather substantial. Ions with the symmetric configurations of their d-orbitals become chemically inactive and similar to noble gases.

Since, according to the Jahn–Teller effect [1–5], TMs (e.g., Pd, Cu, and Zn) often crystallize into clusters with a lowered symmetry, Cu^{2+} and Pd^{5+} ions in the octahedral configuration do not have a completely filled d-shell any more. In other words, the number of electrons in their d-shell is $N_d < 10$. The d^9-bond becomes elongated along the axis Z. Hence, the d^9-bond becomes less screened, so that its reaction ability strongly increases. Therefore, if a d^{10}-ion (with spherical symmetry) is reaction-passive, the d^{10-n}-ion has a "vacancy" in its d-shell, which is responsible for its chemical activity.

Similar modifications in the electron configuration of TMs also take place in complexes with active acceptor impurities such as O, S, Cl, F, Br, In, and others. In particular, for the tetragonal structure of Cu with acceptor impurities (Cl_2, Br_2, J_2), d^9-ions are formed, whose structure includes two long (≈0.3 nm) reaction-active d_{Z^2} orbitals and four short (≈0.23 nm) $d_{x^2-y^2}$ ones. The degeneration is eliminated, the d-levels become split, and the structure becomes additionally stabilized in the crystalline field [2]. Structures with two long and four short bonds, which are similar to d^9 according to works [2–5], are met in high-spin complexes of ions with weakly filled d-orbitals: d^4-($Cr^{2+}Mn^{7+}$) and d^7-($Co^{2+}N_1^{3+}$) shells.

The theoretical molecular orbital method, together with the crystalline field theory, makes it possible to calculate the cluster parameters on the basis of the term energies of atomic cluster components with the regard for the symmetry of a molecular structure, by proceeding from the data available for atomic radii [6–11]. In order to evaluate the chemical activity of nanoclusters, the contributions of the polar (ε_i) and valence (ε_v) components of the chemical bond are calculated. This is those components that determine whether the electron configuration can be changed or not. Using the known data for the atomic electron terms (ε_v, ε_m, and ε_i) and selecting a geometry for the structural configuration of atomic components in the nanocluster created owing to inter-orbital transitions, the energy of a chemical bond can be calculated (Table 1).

Figure 3 shows a schematic energy diagram, which illustrates changes in the electron occupation of various orbitals in the clusters with the participation of an acceptor oxygen impurity in CuO and Cu_2O. For those compounds, the 6-eV difference between the level energies for oxygen ($E = -14$ eV) and copper ($E = -20$ eV) prohibits the transition of copper d-electrons onto the oxygen p-level. In this case, for a catalytically active cluster to be formed, the crystalline field has to be large enough to shift the d-level by 6 eV (provided that the transition of a d-electron from shallower (-7 eV) 4s-levels of copper atoms is prohibited). In other words, the formation of a copper ion with the orbital configurations d^8 and d^9 is supposed. Such structures of the copper ion with the incompletely filled d-shells are already chemically active.

There are TMs of two kinds: 1) TMs with completely filled d-orbitals; they are located to the right from the center of the Periodic system; they are described in terms of localized electron states (e.g., copper and its oxides); and 2) TMs with incompletely filled d-orbitals (d^3–d^7) and located to the left from the center of the Periodic system; they form a d-band, which can be calculated, by using the LCMO method with regard for the hybridization of d-orbitals with s- and p-shells [2, 20–22]. It should be emphasized that the energy of d-orbitals in such TMs are comparable with the energies of s- and p-orbitals, which is important for electron transitions $d \Leftrightarrow (s, p)$.

3. Experimental Part

3.1. Specimen preparation and experimental technique

Gas-sensitive metal-insulator-semiconductor (MIS) specimens are studied. They were fabricated on the basis of nanoporous silicon doped with catalytically active Pd and Cu nanoparticles, and Cu–Pd and WO_3–Pd composites (Fig. 4). For the creation of a nanostructured catalytically active composite, a layer of porous silicon with metal clusters, both built-in into pores and deposited on the surface, was used. Layers of porous silicon were formed by electrochemically etching the single-crystalline wafers of silicon (c-Si) with the orientation (100) doped with boron ($N_A = 4 \times 10^{15}$ cm^{-3}) at the current density $j = 5\div30$ mA/cm^2 in a solution of fluoric acid

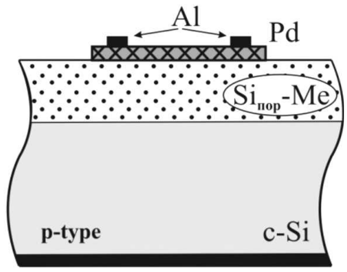

Fig. 4. Schematic diagram of a gas-sensitive structure with a layer of porous silicon and built-in clusters of catalytically active metal

(HF, 48%) and ethyl alcohol C_2H_5OH taken in a ratio of 4 : 1. In order to stabilize their electrophysical parameters, those structures were thermally treated at a temperature of 550 °C for 1 h in the artificial air environment N_2(20%)–O_2(80%). The purity grade of N_2 and Ar was about 99.987%. This treatment resulted in the partial oxidation of the porous silicon surface.

Composite films Cu-Pd and WO_3/Pd were formed on the surface of oxidized nanoporous silicon within the magnetron sputtering method. For the composites to be formed, palladium (≈50 nm), copper (≈5 nm), and tungsten (≈5 nm) films were consecutively deposited onto the surface. We also fabricated structures, in which pores were filled with copper nanoclusters from the 0.5 M aqueous solution of Cu_2SO_4 with the help of the electrolysis method.

Adsorption isotherms were studied in the gas concentration intervals 5–1000 ppm ($1\times10^{-3}\div1$ mm Hg) for hydrogen and 3–100 ppm ($3 \times 10^{-3}\div1 \times \times 10^{-2}$ mm Hg) for hydrogen sulfide in air or the nitrogen environment. The measurements were performed at room temperature, by using the method of high-frequency capacitance-voltage characteristics. The shift of the capacitance at the flat band level, C_{FB}, under the influence of adsorbed hydrogen (H_2) or hydrogen sulfide (H_2S) molecules was measured. In accordance with the expression for the adsorption isotherm $PV = N_a kT$, this shift is proportional to the concentration of adsorbed molecules.

The thicknesses of the nanoporous silicon, palladium, and copper layers were determined with the help of a profilometer Dektak 3030 Auto II. The surface morphology of composites on the basis of porous silicon matrix and Cu, Pd, and WO_3 nanoparticles was studied by the atomic force microscopy (AFM) and scanning electron microscopy (SEM).

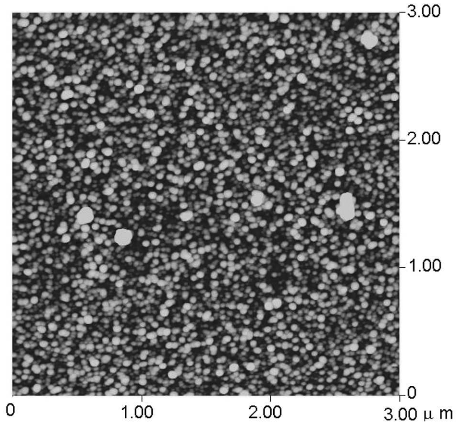

Fig. 5. AFM image of a porous-Si surface with a catalytically active Pd film (for the analysis of the Pd-porSi surface roughness)

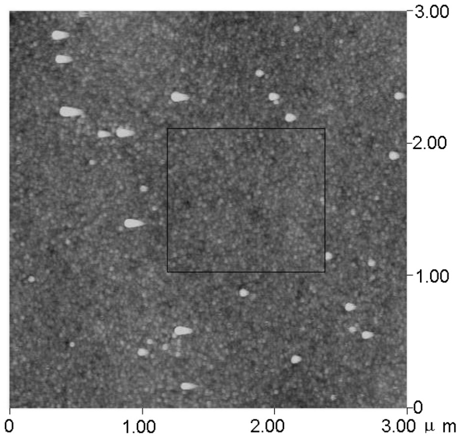

Fig. 6. AFM image of a porous-Si surface with a catalytically active Cu–Pd film (for the analysis of the Cu–Pd-porSi surface roughness

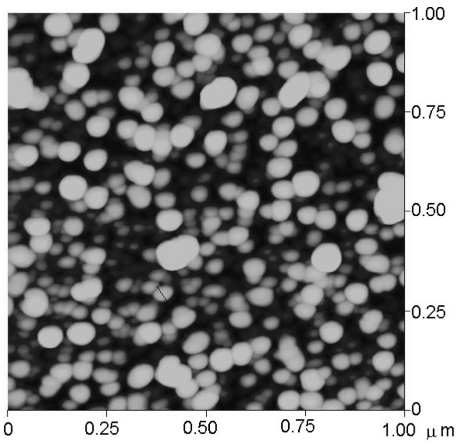

Fig. 7. AFM image of a porous-Si surface with a catalytically active WO_3-Pd film

3.2. AFM and SEM researches of the surface morphology

The results of AFM researches concerning the morphology of the surface of Pd, Cu-Pd, and WO_3–Pd composites are shown in Figs. 5 to 7, respectively. Since the films of composites were formed on the surface of porous Si, which had a complicated relief, they were nanostructured and not continuous. The average size of Cu nanoparticles amounted to 60 ± 20 nm (Fig. 6), and the average size of WO_3 nanoparticles was 50 ± 30 nm (Fig. 7). The small spread of the sizes of Cu and WO_3 nanoparticles can be associated with the fact that nanoporous silicon has pores with an average size of 2–8 nm, i.e. its surface has a uniform roughness (Ra).

The analysis of the surface roughness of a Pd film about 50 nm in thickness formed on the porous Si surface showed that its roughness equaled about 5.7 nm (Fig. 5). However, after a Cu layer about 10 nm in thickness had been deposited onto the surface of a nanostructured Pd film, the surface of the composite Cu-Pd film became more even. Its roughness decreased by more than an order of magnitude in comparison with the roughness of a Pd film and amounted to $Ra \approx 0.4$ nm (Fig. 6).

3.3. Research of electroadsorption on specimens with porous surface

When a fine-grained solid is placed into a closed volume filled with gas, the former starts to actively adsorb this gas. The adsorption is driven by a force field that arises near the solid surface (the adsorbent), which attracts gas molecules (the adsorbate). In general, the attraction forces created by a solid can be of two types: physical and chemical. They are responsible for either the physical (van der Waals) adsorption or chemisorption, respectively. Forces responsible for the physical adsorption always include the dispersion forces – which, by their nature, are attractive forces – and short-range repulsive forces [1, 2, 11–14]. In addition, the adsorption forces should be appended by forces emerging due to constant dipole moments of adsorbed molecules [19, 21, 22].

At the chemisorption, electrons transit between the solid and adsorbed molecules, so that a chemical compound is formed in a thin layer of atoms or molecules on the solid surface. The chemisorption engages the valence, ionic, and other binding mechanisms with a high enough binding energy (>1–2 eV). In order to distinguish between physical adsorption and chemisorption, a number of experimental criteria were proposed. The most known of them is the adsorption heat. At the chemisorption, this parameter is much larger than at the physical adsorption ($\leq$0.1÷0.2 eV).

The adsorption isotherms of hydrogen sulfide, hydrogen, and water were measured at room temperature for gas-sensitive structures with catalytically active composite films on the surface. The specimens were fabricated on the basis of nanoporous silicon matrices with palladium, tungsten oxide, copper, and copper oxide clusters obtained by the magnetron sputtering and built-in into the pores. The concentration of hydrogen sulfide in nitrogen or air changed within the interval 3–150 ppm, which simulated a sensor to work under environmental conditions. Typical results obtained are depicted in Figs. 8 to 10.

The isotherms were analyzed on the basis of the Freundlich theory. The latter gives different initial slopes and power exponents m in the dependence $n_a(p)$ for the ordinary molecular ($n = 1$) and decomposition ($n = 0.5$) processes in the case of homogeneous surface:

$$n_a/N_{\max} = p^m/(1 + p/p^*)^m, \quad (6)$$

where n_a is the number of molecules adsorbed by adsorption centers, $N_{\max}$ the total number of different adsorption centers, p the gas pressure in the measuring chamber, $p^* = B/A\ e^{\varepsilon_a/kT}$ is a characteristic pressure, at which the adsorption magnitude equals half of the possible maximum, ε_a the adsorption heat, $B = 1/\tau_0 = VC_aN$ is the probability of the molecule evaporation at the temperature growth, and $A = (V/4kT)C_a$ is the cross-section of the molecule capture by an adsorption center [3, 4].

In Fig. 8, the adsorption isotherms for hydrogen sulfide dissolved in air are shown. They were obtained, by using gas-sensitive structures with various electrode types: WO_3–Pd–porSi (curve *1*) and Pd–porSi (curve *2*). The approximations of those isotherms by the Freundlich equation (6) at various m-values ($m = 1$ or 0.5) demonstrated a good agreement at relatively high pressures in the case $m = 0.5$ and at low pressures in the case $m = 1$. This fact testifies that the molecule of hydrogen sulfide undergoes the decomposition at high H_2S pressures

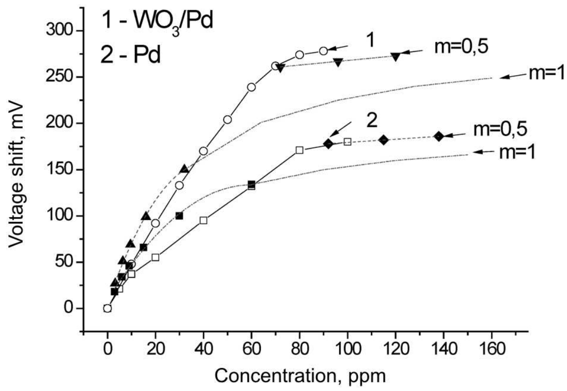

Fig. 8. Dependence of the response signal of a gas-sensitive structure with a porous silicon layer and a nanostructured film of WO_3–Pd composite (*1*) or a Pd film (*2*) under the action of hydrogen sulfide. The dashed curves are the corresponding theoretical curves (Freundlich isotherms)

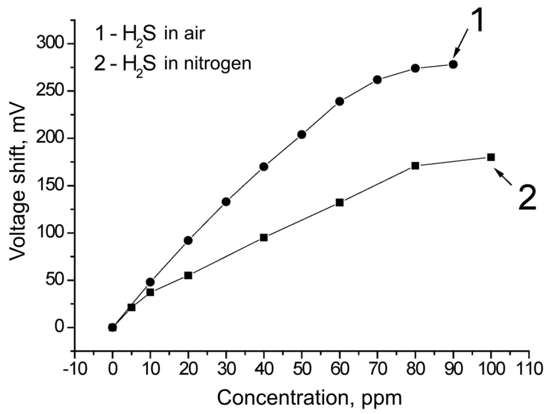

Fig. 9. Dependence of the response signal of a gas-sensitive structure with a porous silicon layer and a nanostructured Pd film under the action of hydrogen sulfide in air (*1*) and nitrogen (*2*)

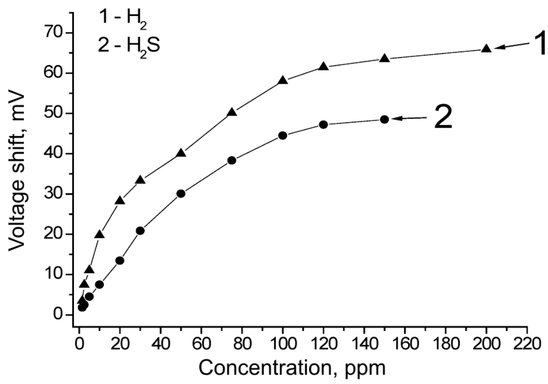

Fig. 10. Dependence of the response signal of a gas-sensitive structure with a porous silicon layer and a nanostructured Pd film under the action of hydrogen (*1*) and hydrogen sulfide (*2*)

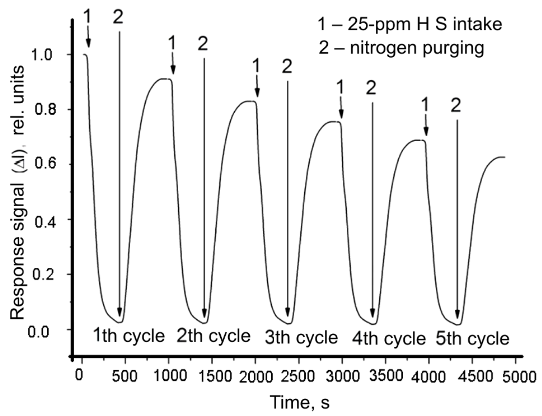

Fig. 11. Reproducibility of the response signal produced by the Al–Cu /porSi–Si structure under the influence of hydrogen sulfide (25 ppm) during five cycles

Table 2. **Adsorption energies for H_2S and H_2 in their mixtures with N_2, air, and H_2O**

N/N	Structure	Gas	ε_a, eV
1	Cu/Pd/porSi	H_2S/N_2	0.530
2	Cu/Pd/porSi	H_2S/air	0.528
3	WO_3/Pd/porSi	H_2S/N_2	0.589
4	WO_3/Pd/porSi	H_2S/air	0.582
5	Cu (el.)/porSi	H_2S/air/H_2O (1 ML)	0.561
6	Cu (el.)/porSi	H_2S/air/H_2O (2 ML)	0.509
7	Cu/Pd/porSi	H_2S/N_2	0.532
8	Pd/porSi	H_2S/N_2	0.538
9	Cu (el.)/porSi	H_2S/N_2	0.548
10	Cu/Pd/porSi (Annealing: 150° C, 25%O_2–75%N_2, 60 min)	H_2/N_2	0.375

($p > 80$ ppm), whereas hydrogen sulfide is absorbed in the molecular form at low pressures ($p < 25$ ppm).

The sensitivity of the structures with WO_3–Pd–porSi composites with respect to H_2S in air is higher than that of the structures with Pd–porSi. The voltage shift at the U_{FB} level for a H_2S concentration of 30 ppm in air amounts to 220 mV for the sensitive WO_3–Pd–porSi layer (*1*), which is more than for the Pd–porSi layer (≤180 mV, *2*). This is a result of the fact that, when an H_2S molecule is adsorbed on the surface of a WO_3 oxide cluster, it is decomposed, which gives rise to a large enhancement of the H_2S sensitivity. If H_2S interacts with the electrode for a long time, there appears a sulfur layer on the electrode surface.

Furthermore, the sensitivity of the examined sensitive structures to hydrogen sulfide in air and at room temperature was higher in comparison with their sensitivity to hydrogen sulfide in nitrogen. In particular, the shift of the flat-band voltage under the influence of adsorbed hydrogen sulfide at a level of 30 ppm for H_2S in air is equal to about 150 mV, and to about 100 mV for H_2S in nitrogen (Fig. 8). In the framework of the theoretical concept for the enhanced absorption-catalytic activity of composites with transition metals, which was described above [2, 3], it was shown that the adsorbed molecules of donor or acceptor gases (O_2, Cl_2, F) and oxide compounds on the surface of catalytic composites can favor the decomposition of adsorbed molecules and a drastic enhancement of their chemical activity. The latter occurs due to the elimination of the *d*-orbit degeneration and the splitting of this orbit under the action of a crystalline field into two bands, e_g (two levels, $d_{x^2-y^2}$ and d_{z^2}, with a higher energy) and t_{2g} (three levels, d_{xy}, d_{xz}, and d_{yz}, with a lower energy). This process can explain the enhanced sensitivity of the structures concerned with respect to the adsorption of H_2S in air (a mixture), O_2, H_2O, and other environments in comparison with the sensitivity in an inert gas (N_2).

We also performed a cycle of works aimed at researching the adsorption isotherms of hydrogen sulfide and hydrogen in air on the structures with catalytically active Pd–porSi electrodes at room temperature (Fig. 10). The structures with Pd–porSi films turned out more sensitive to hydrogen than to hydrogen sulfide. The mechanism of enhanced sensitivity to H_2 on Pd–porSi composites consists in the facilitated dissociative adsorption of H_2 molecules on the surface of Pd clusters, rapid diffusion of hydrogen atoms toward the Pd/SiO_2 interface, and their polarization under the influence of the field created by the contact potential difference Pd–Si. The additional field of dipoles results in a reduction of the Pd work function and in a shift of the C–V curve proportionally to the H_2 concentration in air. When H_2S molecules are adsorbed on the surface of Pd clusters, the level of their dissociation is less in comparison with that for H_2, which can explain the high sensitivity of the examined structures to the adsorption of H_2 molecules [23–25].

Our research of the electroadsorption effect kinetics for H_2S molecules testifies to a substantial reproducibility of this effect within the limit of 20% and an almost complete recovery of the initial values during several cycles (Fig. 11). A large number of cycles and a high pressure give rise to the appearance of a thin sulfur layer on the surface. For its removal and the structure sensitivity restoration, thermal treatments at moderate temperatures for 30 min in the hydrogen atmosphere were applied. These results testify that the mechanism of physical adsorption is realized within short time intervals, whereas the chemical adsorption within long and very long ones. This conclusion agrees with the calculation results obtained for the adsorption isotherms. They give values of about 0.3–0.5 eV, which are typical of the physical adsorption with a moderate binding energy (see Table 2).

4. Conclusions

The results obtained allow us to draw the following conclusions. Nanostructured catalysts of a new type fabricated on the basis of nanoclusters of transition metals (W, Pd, Cu) and their oxides are characterized by an enhanced activity with respect to the adsorption and catalytic decomposition of H_2S, H_2, and H_2O molecules. The important components of this mechanism are as follows: the presence of partially filled *d*-orbitals and the nanocluster structure of transition metals, which favors an enhancement of the catalytic activity of TM composites at their interaction with acceptor oxygen atoms.

The work was executed in the framework of the following projects of the National Academy of Sciences of Ukraine: No. 23-2017 (the complex scientific and engineering program of the NASU "Sensor devices for medico-ecological and industry-technological needs: metrological support and test exploitation", the head of the program is Academician G.V. Yelska), No. III-5-16 "Photoelectric and structural characteristics of doped nanosized semiconductor materials", and No. III-10-15 "Development of methods for fabrication and metrological support of complex semiconductor and instrument structures".

1. F.F. Volkenshtein, *The Electronic Theory of Catalysis on Semiconductors* (Pergamon Press, 1963).
2. V.F. Kiselev, O.V. Krilov. *Adsorption and Catalysis on Transition Metals and Their Oxides* (Springer, 1989).
3. V.G. Litovchenko, Electroadsorption effects in layered systems insulator-semiconductor. *Zh. Fiz. Khim.* **52**, 3063 (1978).
4. *Advanced Sensor and Detection Materials,* edited by A. Tiwari, M.M. Demir (Wiley, 2014).
5. G. Bozzolo, J.E. Garces, R.D. Noebe, P. Abel, H.O. Mosca. Atomistic modeling of surface and bulk properties of Cu, Pd and the Cu–Pd system. *Prog. Surf. Sci.* **73**, 79 (2003).
6. W.A. Harrison, *Solid State Theory* (McGraw-Hill, 1970).
7. J.C. Bertolini, P. Miegge, P. Hermann, J.L. Rousset, B. Tardy. On the reactivity of 2D Pd surface alloys obtained by surface segregation on deposition technique. *Surf. Sci.* **331**, 651 (1995).
8. J. Greeley, J.K. Norskov. A general scheme for the estimation of oxygen binding energies on binary transition metal surface alloys. *Surf. Sci.* **592**, 104 (2005).
9. N. Lopez, T.V.W. Janssens, B.S. Clausen, Y. Xu, M. Mavrikakis, T. Bligard, J.K. Norskov. On the origin of the catalytic activity of gold nanoparticles for low-temperature CO oxidation. *J. Catal.* **223**, 232 (2004).
10. A. Nilsson, L.G.M. Petersson, B. Hammer, T. Bligaard, C.H. Christensen, J.K. Norskov. The electronic structure effect in heterogeneous catalysis. *Catal. Lett.* **3–4**, 111 (2005).
11. V.G. Litovchenko, T.I. Gorbanyuk, O.O. Yefremov, A.A. Yevtukh, Yu.G. Ptushinskyy, V.A. Ischuk, O.V. Kanash. Catalytic peculiarities of ultra-thin palladium films and its alloys. *Ukr. Fiz. Zh.* **48**, 565 (2003) (in Ukrainian).
12. V.G. Litovchenko, V.S. Solntsev. Sensing effects in the nanostructured systems. In *Proceedings of the NATO Advanced Research Workshop on Electron Transport in Nanosystems* **22**, 373 (2008).
13. V.G. Litovchenko, T.I. Gorbanyuk, V.S. Solntsev. New adsorption active nanoclusters for ecological monitoring. In *Nanodevices and Nanomaterials for Ecological Security – NATO for Peace and Security. Series B: Physics and Biophysics* (Springer, 2012), p. 297.
14. J. Kukkola, J. Moklin, N. Halonen *et al.* Gas sensors based on anodic tungsten oxide. *Sens. Actuat. B* **153**, 293 (2011).
15. A.K. Nayak, R. Ghosh, S. Santra, P.K. Guha, D. Pradhan. Hierarchical nanostructured WO_3–SnO_2 for selective sensing of volatile organic compounds. *Nanoscale* **7**, 12460 (2015).
16. *Synthesis, Properties, and Applications of Oxide Nanomaterials*, edited by J.A. Rodriguez, M. Fernández-García (Wiley, 2007).
17. V.G. Litovchenko, T.I. Gorbanyuk, V.S. Solntsev, A.A. Evtukh. Mechanism of hydrogen, oxygen and humidity sensing by Cu/Pd-porous silicon–silicon structures. *Appl. Surf. Sci.* **234**, 262 (2004).
18. V.G. Litovchenko, T.I. Gorbanyuk, A.A. Efremov, A.A. Evtukh, D. Schipanski. Investigation of MIS gas sensitive structures with Pd and Pd/Cu metal layers. *Sens. Actuat. A* **74**, 233 (1999).
19. R.S. Niranjan, V.A. Chaudhary, I.S. Mulla, K. Vijayamohanan. A novel sulfide room sensor based on copper nanocluster functionalized tin oxide thin films. *Sens. Actuat. B* **85**, 26 (2002).
20. A. Ruban, B. Hammer, P. Stoltze, H.L. Skriver, J.K. Norskov. Surface electronic structure and reactivity of transition and noble metals. *J. Mol. Catalys. A* **115**, 421 (1997).

21. A.I. Manilov, V.A. Skryshevsky. Hydrogen in porous silicon – A review. *Mater. Sci. Eng. B* **178**, 942 (2013).
22. T.I. Gorbanyuk, A.A. Evtukh, V.G. Litovchenko, V.S. Solntsev. Porous silicon microstructure and composition characterization depending on the formation conditions. *Thin Solid Films* **495**, 134 (2006).
23. O.L. Syshchyk, V.A. Skryshevsky, O.O. Soldatkin, A.P. Soldatkin. Enzyme biosensor systems based on porous silicon photoluminescence for detection of glucose, urea and heavy metals. *Biosens. Bioelectron.* **66**, 89 (2015).
24. A.I. Manilov, S.A. Alekseev, V.A. Skryshevsky, S.V. Litvinenko, G.V. Kuznetsov, V. Lysenko. Influence of palladium particles impregnation on hydrogen behavior in meso-porous silicon. *J. Alloys Comp.* **492**, 466 (2010).
25. M.S. Shivaraman. Detection of H_2S with Pd-gate MOS field-effect transistors. *J. Appl. Phys.* **47**, 3591 (1976).

Received 24.06.16.
Translated from Ukrainian by O.I. Voitenko

В.Г. Литовченко, Т.І. Горбанюк, В.С. Солнцев

МЕХАНІЗМ АДСОРБО-КАТАЛІТИЧНОЇ АКТИВНОСТІ НАНОСТРУКТУРОВАНОЇ ПОВЕРХНІ КРЕМНІЮ, ЛЕГОВАНОЇ КЛАСТЕРАМИ ПЕРЕХІДНИХ МЕТАЛІВ ТА ЇХ ОКСИДАМИ

Р е з ю м е

Проведено теоретичний аналіз механізмів адсорбо-каталітичної активації композитів, виготовлених на основі поруватого кремнію з інкорпорованими наночастинками перехідних металів (Pd, W, Cu) та їх оксидів. Встановлено вплив адсорбованих атомів акцепторних елементів (O, S, F, Cl) на каталітичну активність перехідних металів при формуванні поверхневих нанокластерів оксидів перехідних металів. Механізм підвищення каталітичної активності перехідних металів з повністю заповненою d-зоною, імовірно, може полягати в зміні заповнення електронами d-станів (появі d-дірок над рівнем Фермі) при утворені поверхневих нанокластерів оксидів перехідних металів. Представлено результати експериментальних досліджень адсорбо-електричного ефекту методом високочастотних вольт-фарадних характеристик газочутливих структур з бар'єрами Шоттки, які характеризують дані процеси. Проведено аналіз експериментальних ізотерм адсорбції водню та сірководню на поверхні наноструктурованих композитів кремнію з нанокластерами міді, вольфраму, паладію та їх оксидів в порах. Було виявлено підвищену адсорбційну чутливість даних композитів до різних газів (H_2, H_2S, H_2O) в порівнянні зі звичайним поруватим шаром кремнію. Встановлено, що при низьких тисках газу ($\geq$25 ppm) та/або при малих часах взаємодії адсорбат-підкладка реалізується механізм фізичної адсорбції, а при більш високих тисках та довготривалих процесах – хемосорбції. Цей висновок узгоджується з даними, отриманими з розрахунків теплоти адсорбції по експериментальним ізотермам, які дають значення 0,3–0,5 еВ.